JOURNAL OF PHYSICAL ORGANIC CHEMISTRY
J. Phys. Org. Chem. 2004; **17:** 665–674
Published online in Wiley InterScience (www.interscience.wiley.com). DOI: 10.1002/poc.836

Phenol radical cations and phenoxyl radicals in electron transfer from the natural phenols sesamol, curcumin and trolox to the parent radical cations of 1-chlorobutane

R. Joshi,[1] S. Naumov,[2] S. Kapoor,[1] T. Mukherjee,[1] R. Hermann[3] and O. Brede[3]*

[1]Radiation Chemistry and Chemical Dynamics Division, Bhabha Atomic Research Center, Mumbai 400085, India
[2]Leibniz Institute of Surface Modification, Permoserstrasse 15, 04303 Leipzig, Germany
[3]Interdisciplinary Group Time Resolved Spectroscopy, University of Leipzig, Permoserstrasse 15, 04303 Leipzig, Germany

Received 11 March 2004; accepted 26 April 2004

ABSTRACT: The free electron transfer from sesamol, curcumin and trolox to solvent (1-chlorobutane) radical cations was studied. The solutes (ArOH) react with $BuCl^{\cdot+}$ at diffusion-controlled rates ($\sim 10^{10}\,dm^3\,mol^{-1}\,s^{-1}$) resulting, simultaneously, in phenol-type radical cations ($ArOH^{\cdot+}$) and phenoxyl radicals ($ArO^{\cdot}$) with an $ArOH^{\cdot+}/ArO^{\cdot}$ ratio >1. It was found that the kinetics are markedly affected by the different substituents on the aromatic ring of $ArOH^{\cdot+}$. The various $ArOH^{\cdot+}$ react with triethylamine with rate constants of $\sim 10^9\,dm^3\,mol^{-1}\,s^{-1}$, whereas ethanol and dioxane are ineffective as cation scavengers. The effect of substituents on the electron transfer and the $ArOH^{\cdot+}/ArO^{\cdot}$ ratio is discussed on the basis of experimental data and quantum chemical calculations. Copyright © 2004 John Wiley & Sons, Ltd.

KEYWORDS: electron transfer; radical cations; sesamol; curcumin; trolox; kinetics; non-polar solvents; phenoxyl radicals

INTRODUCTION

Radical cations appear as primary products in a variety of processes such as one-electron oxidations, photosensitized electron transfer (ET) and radiation-induced reactions.[1,2] Radiation-induced reactions in non-polar solvents offer a convenient way to produce radical cations of a variety of solutes through ET.[3,4] In non-polar solvents, such as 1-chlorobutane (BuCl) (ionization potential, $IP_g = 10.67\,eV$), the radiation generated solvent radical cations ($BuCl^{\cdot+}$) [reaction (1)] react at diffusion-controlled rates with solutes of lower ionization potentials ($IP_g \leq 10.6\,eV$) [reaction (2)].[5,6] The alkyl chloride radical cations (σ-type) are metastable species, stabilized by the nearly uniform distribution of charge over the molecule. Furthermore, the very high free energy (corresponding to the gas phase solute–solvent ionization potential difference of $\sim 2\,eV$) of the ET in non-polar systems results in a non-hindered and rapid generation of solute radical cations ($ArOH^{\cdot+}$) as described by reaction (2), which is explained in detail subsequently in this paper.

$$BuCl \quad -vvvv \rightarrow \quad BuCl^{\cdot+}, Cl^{-}, \text{ radicals, etc.} \quad (1)$$

$$BuCl^{\cdot+} + ArOH \rightarrow ArOH^{\cdot+} + BuCl \quad (2)$$

**Correspondence to:* O. Brede, Interdisciplinary Group Time Resolved Spectroscopy, University of Leipzig, Permoserstrasse 15, 04303 Leipzig, Germany.
E-mail: brede@mpgag.uni-leipzig.de

Because of kinetic pecularities, reaction (2) is named free electron transfer (FET). After the encounter of the reactants, the electron jump proceeds extremely rapid on a time scale comparable to or even shorter than molecular motions.[7–13] Experimental evidence suggests that FET from phenols (ArOH) to $BuCl^{\cdot+}$ results in a simultaneous generation of phenol radical cations ($ArOH^{\cdot+}$) as well as phenoxyl radicals ($ArO^{\cdot}$), in comparable amounts.[7]

The simultaneous formation of radical cation and radical has been attributed to the unhindered continous rotation of the phenolic OH group with respect to the aromatic ring in the singlet ground state. Two borderline situations can be envisaged, **3a** and **3b**.

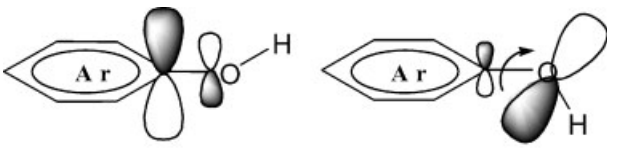

3(a) **3(b)**

The rotation of the phenolic OH group is accompanied by changes in the electron density distribution over the molecule, i.e. over its high orbital levels. Relatively seen, the molecular oscillations are much faster than the motions by diffusion. Hence FET is virtually differentiating between the diversity of all imaginable rotamers, i.e. different angles of OH vs the aromatic ring. For simplification,

in our treatment the electron transfer from these rotamers is viewed for two extreme cases with the OH group in the molecular plane (cf. **3a**) and perpendicular to the molecular plane (cf. **3b**). Each situation results in the formation of two kinds of a specific product, either a long-living radical cation [Eqn (4a)] or a very short-living (non-observable) and immediately dissociating radical cation [Eqn (4b)], respectively.[7]

$$\mathrm{ArOH_{in\text{-}plane}} \rightarrow \quad [[\mathrm{ArOH}]^{\cdot+}]^{*} \rightarrow \quad \mathrm{ArOH}^{\cdot+} \qquad (4a)$$

$$\mathrm{BuCl}^{\cdot+} + \quad \downarrow\uparrow \qquad\qquad + \mathrm{BuCl}$$

$$\mathrm{ArOH_{perpendicular}} \rightarrow \; [\mathrm{ArO}^{\cdot+} - \mathrm{H}]^{*} \rightarrow \quad \mathrm{ArO}^{\cdot} + \mathrm{H}^{+} \qquad (4b)$$

Hetero groups of different types influence the observed ratios between cation radical and radical. In the present work, electron transfer from some natural phenolic compounds, sesamol [3,4-(methylenedioxy)phenol], curcumin [1,7-bis(4-hydroxy-3-methoxyphenyl)-1,6-heptadiene-3,5-dione] and the α-tocopherol analog trolox (6-hydroxy-2,5,7,8-tetramethylchroman-2-carboxylic acid) (Scheme 1) to $\mathrm{BuCl}^{\cdot+}$ and benzene radical cations has been investigated. These phenols possess substituents which influence the electronic structure of the molecule and cause special steric and H-bonding phenomena, providing stabilization of transients, and therefore could affect reaction kinetics. Scavenging of $\mathrm{ArOH}^{\cdot+}$ of sesamol, curcumin and trolox with dioxane, ethanol and triethylamine for transient identification has also been studied.

EXPERIMENTAL

Pulse radiolysis

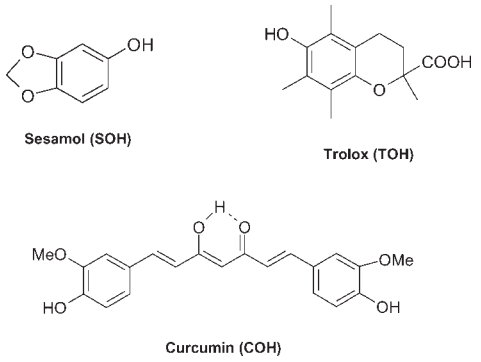

Scheme 1

The samples were irradiated with a high-energy (1 MeV) electron beam of 15 ns pulse duration generated by a pulse transformer electron accelerator ELIT (Institute of Nuclear Physics, Novosibirsk, Russia). The dose per pulse was measured using the absorbance of the solvated electron in slightly alkaline solution. The experiments were carried out at 100 Gy, which generates about 2×10^{-5} mol dm^{-3} of $\mathrm{BuCl}^{\cdot+}$ as primary oxidants. Transient species formed were detected by the optical absorption technique, in our case consisting of an XBO 450 W pulsed xenon lamp (Osram), a SpectraPro-500 monochromator (Acton Research), an R955 photomultiplier (Hamamatsu Photonics) and a TDS 640 1 GHz digitizing oscilloscope (Tektronix). Further details of the instrumental setup are given elsewhere.[9,11] All experiments were performed at room temperature using freshly prepared solutions in 1-BuCl purged with purest grade N_2 for 15 min prior to the pulse radiolysis measurements. The solutions were continuously passed through the sample cell with an optical pathlength of 1 cm. The kinetic simulations of the superimposed transient absorption time profiles obtained were performed using our own computer program based on the ACUCHEM procedure,[14] which numerically solves the rate equations for the various transients within the reaction mechanism.

Chemicals

1-Butyl chloride was purified by chromatography using molecular sieve treatment (A4, X13) and distillation under nitrogen. Solvents from VWR were of liquid chromatography grade. The solvent purity was confirmed by UV spectroscopy before use. The solutes sesamol (Fluka, 98%), curcumin (Fluka, 95%) and trolox (Sigma, 98%) were of the highest commercially available purity and used as received.

Quantum chemical calculations

Quantum chemical calculations were performed with the Gaussian 98 Revision 11 program package[15] using the density functional theory (DFT) hybrid B3LYP[16–18] method. Frequency calculations were performed to determine the nature of stationary points found by geometry optimization and to obtain thermochemical parameters such as zero-point energy and activation energy, E_a (height of rotation barrier).

RESULTS AND DISCUSSION

Pulse radiolysis studies

Sesamol. In the pulse radiolysis of sesamol in 1-chlorobutane, the absorption band of the primary radical cation ($\mathrm{BuCl}^{\cdot+}$) disappears with simultaneous formation of absorption bands of sesamol transients at 320, 425 and 455 nm (Fig. 1) just after the electron pulse. $\mathrm{BuCl}^{\cdot+}$ reacts with sesamol with $k_2 \approx 10^{10}$ dm^3 mol^{-1} s^{-1} as calculated

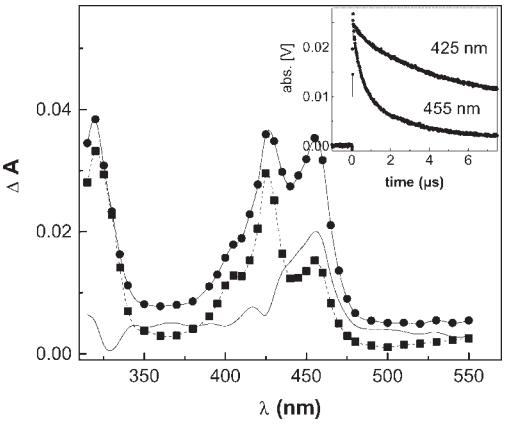

Figure 1. Transient absorption spectra obtained in the pulse radiolysis of an N_2-purged solution of sesamol (2×10^{-3} mol dm^{-3}) in 1-BuCl, 50 ns (●) and 0.7 μs (▲) after the electron pulse. The line gives the difference spectrum between (●) and (▲). Inset: absorption time profiles at 425 and 455 nm under identical conditions

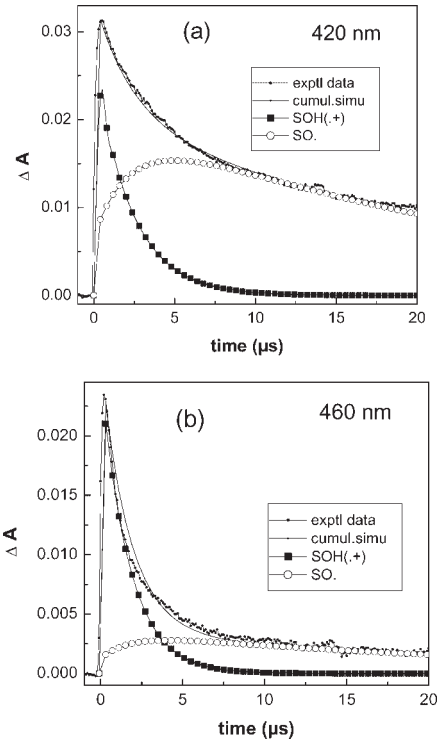

Figure 2. Experimental and simulated time profiles of sesamol transients at (a) 420 and (b) 460 nm obtained in the pulse radiolysis of an N_2-purged solution containing sesamol (5×10^{-3} mol dm^{-3}) in 1-BuCl. 'Cumul.simu' stands for the superposition according to the individual contributions of the transients taken into account

from the decay of $BuCl^{\cdot+}$ at 500 nm for different concentrations; see reaction (2). The transient absorbing at $\lambda_{max} = 455$ nm decays faster than that with an absorption at $\lambda_{max} = 425$ nm, as shown by the respective absorption time profiles given as insets in Fig. 1. Taking into account the spiky rest absorption of $BuCl^{\cdot+}$, the comparatively higher decay rate constant of the absorption at 455 nm suggests that this transient is due to the sesamol radical cation. The difference in the absorption spectra taken at 50 and 700 ns represents the absorption spectrum of the sesamol radical cation with λ_{max} around 455 nm (Fig. 1). The transient absorption at 425 nm is assigned to the sesamol radical ($SO^{\cdot}$), which is known to exhibit an absorption maximum at ~420 nm in aqueous solutions.[19] Because of the overlapping of the absorption bands at 425 and 455 nm, the formation and decay rates of transients could be determined by a kinetic analysis only. Using our kinetic simulation program formation rate constants in the region of 1.5×10^{10} dm^3 mol^{-1} s^{-1} at 455 and 425 nm were obtained. The experimental absorption time profiles of the sesamol transients are compared with numerically calculated concentration vs time profiles, as shown in Fig. 2. As can be seen, the simulations clearly confirm the simultaneous formation of the two species, a phenol-type radical cation ($SOH^{\cdot+}$) and a phenoxyl-type radical ($SO^{\cdot}$). For the whole simulation a set of differential equations was used as described in a later section. The contribution of the $BuCl^{\cdot+}$ absorption at 455 nm is negligible at higher concentrations of sesamol ($\geq 5 \times 10^{-3}$ mol dm^{-3}). Therefore, lifetime estimations were performed for $\geq 5 \times 10^{-3}$ mol dm^{-3} sesamol.

The delayed formation of the phenoxyl is due to the deprotonation of the metastable radical cation:

$$ArOH^{\cdot+}, (BuCl) \rightarrow ArO^{\cdot} + H^{+}(BuCl) \qquad (5)$$

An analogous phenomenon was also observed for thiophenols and selenophenols.[7–13]

Taking into account overlapping of the absorption bands of $SOH^{\cdot+}$ ($\lambda_{max} = 455$ nm) and $SO^{\cdot}$ ($\lambda_{max} = 425$ nm), it was calculated that $SOH^{\cdot+}$ decays with $k = 4.5 \times 10^5$ s^{-1} whereas $SO^{\cdot}$ decays slowly by second-order kinetics with $2k/\varepsilon = 4 \times 10^6$ s^{-1}.

The identification of the sesamol radical cation ($SOH^{\cdot+}$) was further confirmed by adding typical cation radical scavengers such as dioxane, ethanol and triethylamine. The decay rates of transient absorptions are not markedly affected using ethanol ($IP_g = 10.47$ eV) or dioxane ($IP_g = 9.19$ eV)[6]. However, in the presence of ethanol (C_2H_5OH) or dioxane ($C_4H_8O_2$) the yields of the transient absorptions of $SOH^{\cdot+}$ and also of $SO^{\cdot}$ are reduced, caused by the competitive scavenging of $BuCl^{\cdot+}$ [reactions (2) and (6)].

$$C_4H_9Cl^{\cdot+} + C_2H_5OH/C_4H_8O_2 \rightarrow C_2H_5OH_2^{+}/C_4H_9O_2^{+} + C_4H_8Cl^{\cdot} \qquad (6)$$

However, a delayed formation of $SO^{\cdot}$ was observed on addition of dioxane (1 mol dm^{-3}), which indicates for a proton transfer from $BuCl^{\cdot+}$ to dioxane and also from $SOH^{\cdot+}$ to dioxane. The observed transient absorption bands were not influenced by oxygen, in line with the known low

reactivity of radical cations and phenoxyl radicals with oxygen.[7,8] Addition of triethylamine (TEA) with $IP_g = 7.5\,eV$[6] quenches $SOH^{\cdot+}$ (455 nm) with $k_7 = 5 \times 10^9\,dm^3\,mol^{-1}\,s^{-1}$ as given by reaction (7). From the product side ($TEA^{\cdot+}$) and the observed diffusion-controlled rate, an electron transfer quenching is assumed.

$$ArOH^{\cdot+} + TEA \rightarrow TEA^{\cdot+} + ArOH \qquad (7)$$

Furthermore, the electron transfer from phenols to π-type radical cations was studied. For this purpose, a stepwise electron transfer was performed, i.e. from benzene ($IP_g = 9.24\,eV$)[6] to $BuCl^{\cdot+}$ [reaction (8a)] and subsequently from phenol to $C_6H_6^{\cdot+}$ [reaction (9)]. Here, we have to consider that the benzene radical cation exists in a monomer–dimer equilibrium.[20] The electron transfer from ArOH to $C_6H_6^{\cdot+}$ gave similar spectra and transient ratios as described for the $BuCl^{\cdot+}$ solutions (Fig. 3). Also, the decay behaviour of the absorption bands at 455 nm ($SOH^{\cdot+}$) and 425 nm ($SO^{\cdot}$) was found to be similar (see time profiles in Fig. 3), again confirming the transient assignments. For those experiments, the concentration of benzene was up to 100 times that of sesamol.

$$BuCl^{\cdot+} + C_6H_6 \rightarrow C_6H_6^{\cdot+} + BuCl \qquad (8a)$$

$$C_6H_6^{\cdot+} + C_6H_6 \rightleftharpoons (C_6H_6)_2^{\cdot+} \qquad (8b)$$

$$ArOH + C_6H_6^{\cdot+} \rightarrow ArOH^{\cdot+}, ArO^{\cdot} + C_6H_6 \qquad (9)$$

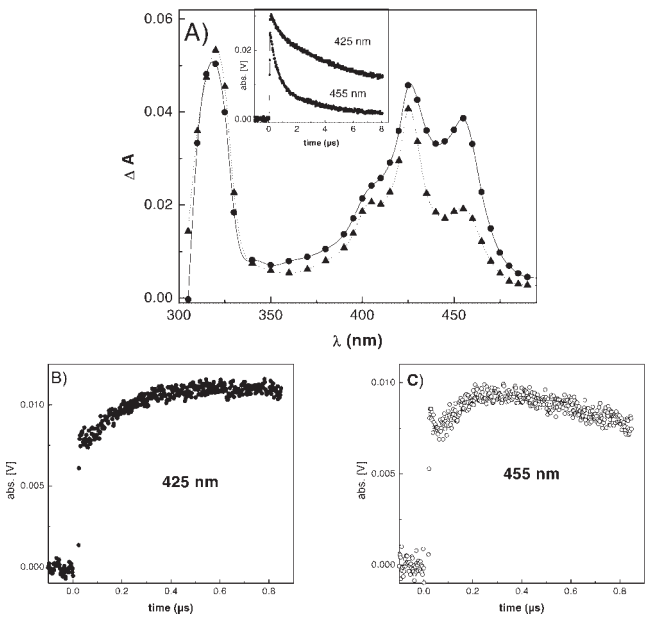

Figure 3. (A) Transient absorption spectrum observed in the pulse radiolysis of an N_2-bubbled solution containing sesamol ($2 \times 10^{-3}\,mol\,dm^{-3}$) and benzene ($5 \times 10^{-1}\,mol\,dm^{-3}$) in 1-BuCl at 60 ns (●) and 0.65 µs (▲) after the electron pulse. Inset: absorption time profiles at 425 and 455 nm taken for decay under same conditions. Formation time profiles at 425 nm (B) and 455 nm (C) taken with $2 \times 10^{-4}\,mol\,dm^{-3}$ sesamol in 1-BuCl

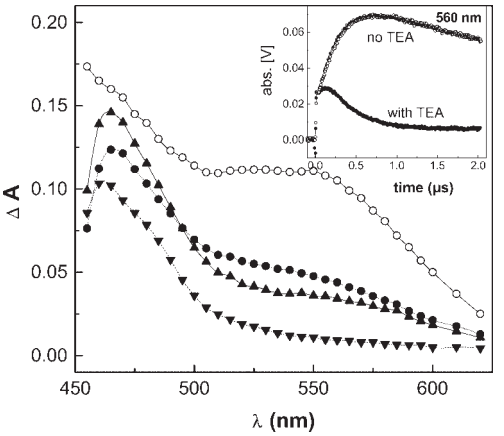

Figure 4. Transient absorption spectra obtained in the pulse radiolysis of an N_2-bubbled solution containing curcumin ($2 \times 10^{-4}\,mol\,dm^{-3}$) in the absence of TEA at 0.44 µs (○) and curcumin ($4 \times 10^{-4}\,mol\,dm^{-3}$) in the presence of TEA ($3.44 \times 10^{-4}\,mol\,dm^{-3}$) in 1-BuCl at 0.14 µs (●), 0.35 µs (▲) and 1.8 µs (▲) after the electron pulse. Inset: absorption time profiles at 560 nm in the presence and absence of TEA under the mentioned conditions

The rate constant for the reaction of $C_6H_6^{\cdot+}$ with SOH as measured by following the pseudo-first-order decay rate of $C_6H_6^{\cdot+}$ was calculated to be $1.6 \times 10^{10}\,dm^3\,mol^{-1}\,s^{-1}$.

Curcumin. COH reacts with $BuCl^{\cdot+}$ (Fig. 4) and $C_6H_6^{\cdot+}$ radical cations to produce transient absorption spectra with maxima at 455 and 560 nm. The transient absorption spectrum could not been studied below 450 nm owing to the COH ground-state absorption. In aqueous media the phenoxyl radical of COH ($CO^{\cdot}$) has been shown earlier to exhibit an absorption maximum around 500 nm.[21] Transient absorptions and kinetics at various wavelengths obtained in the reaction of COH with $BuCl^{\cdot+}$ and $C_6H_6^{\cdot+}$ indicate that the radical cation and the radical derived from COH have broad absorption bands appearing over the whole wavelength range studied. TEA quenches $COH^{\cdot+}$ by electron transfer according to reaction (7) as shown in Fig. 4. The quenching of $COH^{\cdot+}$ (560 nm) is demonstrated by time profiles in the presence and absence of TEA as shown in the inset in Fig. 4. A small depletion effect appears on the 455 nm absorption band. Complete quenching of $COH^{\cdot+}$ at 560 nm could not be achieved because of the competition kinetics reasoned by the low TEA concentration according to the low solubility of curcumin in 1-chlorobutane. The curcumin radical cation reacts with TEA with a rate constant $k_7 = 5.7 \times 10^9\,dm^3\,mol^{-1}\,s^{-1}$ as calculated from the decay of the 560 nm absorptions.

Trolox. As expected, TOH undergoes electron transfer with $BuCl^{\cdot+}$ (Fig. 5) and $C_6H_6^{\cdot+}$ radical cations in an analogous manner as already described for the other phenols. Absorption spectra were obtained (cf. Fig. 5) exhibiting absorption maxima at 320–340, 410 and 460 nm. In aqueous solution at pH 7, it is known that

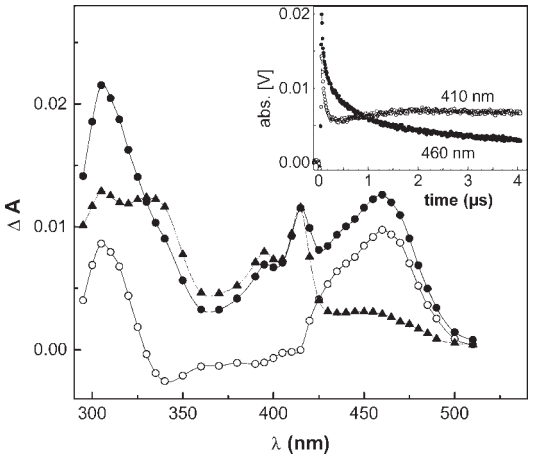

Figure 5. Transient absorption spectrum obtained from an N_2-bubbled solution containing 3.46×10^{-4} mol dm^{-3} trolox in 1-BuCl at 0.5 μs (●) and 7.5 μs (▲) after the electron pulse. (○) Difference spectrum between (●) and (▲). Inset: absorption time profiles of the transients at 410 and 460 nm under the same conditions

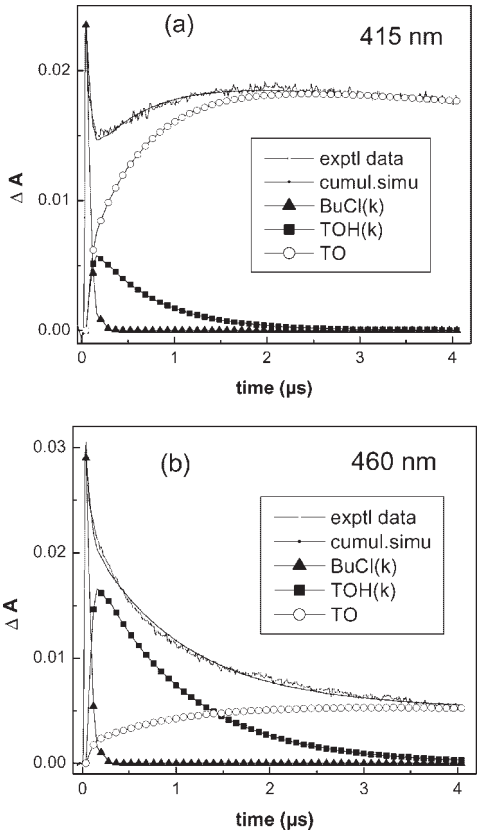

Figure 6. Experimental and simulated time profiles of the trolox transients obtained from an N_2-bubbled solution containing trolox (4×10^{-4} mol dm^{-3}) in 1-BuCl at (a) 415 and (b) 460 nm. 'Cumul.simu' stands for the superposition according to the individual contributions of the transients taken into account

the trolox phenoxyl radical has an absorption maximum around 445 nm.[22] The difference in the absorption spectra taken 0.5 and 7.5 μs after the pulse is shown in Fig. 5, which confirms the assignment of the trolox radical cation with absorption bands at 460 and 305 nm. By analogy with the other phenols, the delayed formation of TO$^{\cdot}$ [see time profiles at 410 nm and reaction (5)] due to the deprotonation of TOH$^{\cdot+}$ is clearly observed for the electron transfer from TOH to both BuCl$^{\cdot+}$ and $C_6H_6^{\cdot+}$. This is demonstrated for the reaction of TOH with BuCl$^{\cdot+}$ by the time profiles at 410 and 460 nm in Fig. 5. Kinetic simulations for 415 and 460 nm are given in Fig. 6. It shows rapid and simultaneous formation of TOH$^{\cdot+}$ and TO$^{\cdot}$ and also delayed formation of a part of TO$^{\cdot}$ within the time-scale where TOH$^{\cdot+}$ decays.

The cation TOH$^{\cdot+}$ decayed with a rate constant $k_7 = 8.5 \times 10^9$ dm^3 mol^{-1} s^{-1} with TEA. Transient absorption spectra and observed time profiles at 410 and 460 nm in the presence of TEA (not shown here) confirm the assignment of TOH$^{\cdot+}$ and TO$^{\cdot}$ according to the absorption maxima at 460 and 410 nm, respectively. The rate constants for the electron transfer inolving SOH, COH and TOH and further kinetic and spectral parameters of the transients investigated are summarized in Table 1. All phenols studied (SOH, COH and TOH) react with BuCl$^{\cdot+}$ and $C_6H_6^{\cdot+}$ to form simultaneously radical cations and phenoxyl radicals in a diffusion-controlled manner. Then, in all cases a delayed deprotonation of the cation radical into the radical takes place. Compared with aqueous systems, in 1-BuCl as solvent the absorption maxima of the phenoxyl radicals of SOH, COH and TOH are blue-shifted by 5, 45 and 25 nm, respectively. The wavelengths of absorption maxima of the radical cations of SOH, COH and TOH have been found to follow the conjugation and electronic effects of the substituents.

Table 1. Rate constants, transient ratio, extinction coefficients used for simulation of the absorption time profiles of the electron transfer from ArOH to BuCl$^{\cdot+}$ and concerned reactions in 1-BuCl (the extinction coefficients were estimated as a result of the kinetic simulation procedure)

Solute	$k_{10a,b}$ (10^{10} dm^3 mol^{-1} s^{-1})	k_{12} (10^6 s^{-1})	$2k_{13}/\varepsilon$ (10^6 s^{-1})	ArOH$^{\cdot+}$/ArO$^{\cdot}$	ε(ArOH$^{\cdot+}$) (dm^3 mol^{-1} cm^{-1})	ε(ArO$^{\cdot}$) (dm^3 mol^{-1} cm^{-1})
SOH	2	0.45	4.0	57/43	4500 (455 nm)	3500 (425 nm)
COH	1	0.30	0.7	62/38	6000 (560 nm)	6500 (455 nm)
TOH	2	1.1	1.3	57/43	5000 (460 nm)	3500 (410 nm)

Simulation of the data

On the basis of experimental data, rate constants for the electron transfer from phenols to $BuCl^{\cdot+}$ or $C_6H_6^{\cdot+}$ and for the deprotonation the of $ArOH^{\cdot+}$ radical cations were determined using kinetic traces at various wavelengths of the transients and at different solute concentrations. Combining these rate constants with reasonable transient extinction coefficients, simulations were performed to obtain the best agreement between calculated and experimental absorption time profiles of all solute transients. On the basis of the assumed reaction mechanism [reactions (10)–(13)], the rate constants given in Table 1 were obtained.

Reaction mechanism

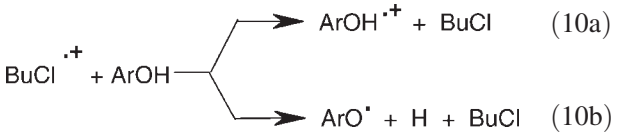

(10a)

(10b)

$$ArOH^{\cdot+} + Cl^- \rightarrow ArO^{\cdot} + HCl \qquad (11)$$

$$ArOH^{\cdot+} + BuCl \rightarrow ArO^{\cdot} + H^+(BuCl) \qquad (12)$$

$$2ArO^{\cdot} \rightarrow \text{product} \qquad (13)$$

The kinetics of the $ArOH^{\cdot+}$ and $ArO^{\cdot}$ species are described by the following differential equations:

$$d[ArOH^{\cdot+}]/dt = k_{10a,b}[ArOH][BuCl^{\cdot+}] - k_{11}[ArOH^{\cdot+}][Cl^-] - k_{12}[ArOH^{\cdot+}] \qquad (14)$$

$$d[ArO^{\cdot}]/dt = k_{10a,b}[BuCl^{\cdot+}][ArOH] + k_{11}[ArOH^{\cdot+}][Cl^-] + k_{12}[ArOH^{\cdot+}] - k_{13}[ArO^{\cdot}]^2 \qquad (15)$$

Representative examples of simulation for sesamol and trolox are shown in Figs 2 and 6, respectively.

The $ArOH^{\cdot+}/ArO^{\cdot}$ ratio

From the described simulations, the ratio $ArOH^{\cdot+}/ArO^{\cdot}$ of the direct formation of $ArOH^{\cdot+}$ and $ArO^{\cdot}$ was determined for all phenols studied. The simulated time profiles for SOH (Fig. 2) and TOH (Fig. 6) show that the radicals ($ArO^{\cdot}$) are formed by a rapid and a delayed time behavior, such as (i) by the immediate deprotonation of the unstable radical cation derived from the perpendicular structure of ArOH [reaction (4b)] and (ii) by time-resolved formation due to the deprotonation of the radical cation in the planar structure [reaction (4a) followed by reaction (12)]. Hence the $ArOH^{\cdot+}/ArO^{\cdot}$ ratio was derived from the fast and from the delayed part of the $ArO^{\cdot}$ radical formation. This reflects the ratio of the transients produced via the two channels of the free electron transfer. The estimated values of the $ArOH^{\cdot+}/ArO^{\cdot}$ ratio for SOH, TOH and COH are 1.3, 1.6, and 1.3, respectively (i.e. the contribution of $ArOH^{\cdot+}$ varies between 57 and 63%).

The phenomenon of the direct generation of solute radical cation ($ArOH^{\cdot+}$) and solute radical ($ArO^{\cdot}$) in the FET has already been described for a number of phenols.[12] In that paper,[12] a ca 1:1 ratio was found for the simultaneous formation of solute radical cations ($ArOH^{\cdot+}$) and solute radicals ($ArO^{\cdot}$) from phenol and phenol derivatives. No influence of the electronic structure of the phenol molecule, which was varied by changing the *para* substitutent (CN, Cl, H, CH_3, OCH_3, etc.), was found. Only for the sterically hindered long tail substituted *n*-octadecyl (3,5-di-*tert*-butyl-4-hydroxyphenyl)propionate a transient ratio $ArOH^{\cdot+}/ArO^{\cdot}$ of 1.12 is given.[8,12] Also within the experimental uncertainties the $ArOH^{\cdot+}/ArO$ ratios for SOH, TOH and COH are higher than those for phenol and its chloro, methoxy, amino and nitro derivatives and even higher than in the case of *n*-octadecyl (3,5-di-*tert*-butyl-4-hydroxyphenyl)propionate.[12] Perhaps, for the case of COH the high $ArOH^{\cdot+}/ArO^{\cdot}$ ratio might be attributed to a high rotational energy barrier, 8.3 kcal mol^{-1} (1 kcal = 4.184 kJ), for the phenolic OH group (Table 2). This may be caused

Table 2. Experimentally obtained lifetime τ of the cation radicals in BuCl compared with DFT B3LYP/6–31G(d)-calculated quantum chemical parameters[a]

Solute	τ (μs)	Log(1/τ)	ν_{Rot} (cm^{-1})	t_{Rot} (10^{-15} s)	ν_{Oscil} (cm^{-1})	t_{Osci} (10^{-15} s)	E_a (kcal mol^{-1})	S(O)	Δq(OH)
Phenol	<0.2	6.7	345	97	3601	9.3	3.0	0.197	0.213
Trolox	0.91	6.04	313	106	3603	9.3	3.9	0.140	0.160
Sesamol	2.22	5.65	325	103	3607	9.2	2.6	0.108	0.150
Curcumin	3.33	5.48	473[b]	70[b]	3546[b]	9.4[b]	8.3	0.058	0.080
			934[c]	36[c]	2848[c]	11.7[c]			

[a] Frequencies (scale factor $f = 0.96$) of polar OH group rotation and valence X—H oscillations; t, times of one motion; E_a, the activation energy of XH group rotation; S(O), atomic spin density at the oxygen; Δq(OH), difference of Mulliken charges at the OH group between cation radical and singlet ground state.
[b] For phenolic OH group.
[c] For enolic OH group.

also by hindrance of the rotation interaction with the neighboring OH and OMe substituents on the aromatic moiety because of an assumed possible hydrogen bridge.

Generally, the data presented in this paper confirm the assumed electron transfer mechanism indicated by the two product lines (10a) and (10b). In addition, evidence is given for further influencing factors such as hydrogen bonding and special rigid molecular structures in the natural phenols SOH, COH and TOH.

Quantum chemical approach

It is known from earlier studies[7–13,20,23,24] that the electron jump within the FET from phenols to solvent (nonpolar) radical cation takes place in $\sim 10^{-15}$ s. This process is faster than the rotational and vibrational motions of the OH group of phenols. Because of the small activation energy (E_a) for the studied molecules, internal rotation of the OH group takes place. Within the Born–Oppenheimer approximation, the molecular geometry is rigid compared with the very fast electron transfer step. The various rotational conformers of the phenols are assumed to be frozen on this time-scale. The electron transfer from these various conformers of phenols can generate different products. Following the same principles as for a variety of simple phenol structures,[7] the rotational motion of the OH group reduces the steric strain in the π-system of the aromatic ring. In a simplification, only two extreme cases of molecular structures arising from the rotation of the OH group have been discussed, namely, the structure with the OH group in the molecular plane and OH perpendicular to it. These structures represent borderline cases and stand for a diversity of rotation situations of the OH group where one category is tending to reaction channel (10a) and the other one to channel (10b). For phenols, in the planar structure the three highest doubly occupied MOs have π-symmetry with strongly delocalized electrons. However, when the OH group is perpendicular to the molecular plane, HOMO and HOMO-1 are delocalized whereas HOMO-2 exhibits n-symmetry and is strongly localized on the oxygen atom of the OH group. This rotational motion changes the electron density and the energy of the HOMOs with an out-of-plane twisting. The HOMO, HOMO-1 and HOMO-2 undergo changes in their energies with out-of-plane twisting which also reduces the separation of these MO levels. Because of the excess energy and the very good orbital overlapping, the electron transfer can take place also from HOMO-2, i.e. from the localized structure. Electron transfer from HOMO-2 produces solute radical cations in an excited state with high spin density on the oxygen atom of the OH group [Equation (4b)]. This is followed by a rapid deprotonation to produce solute radicals within a few femtoseconds. On the other hand, the electron transfer from the other HOMOs of planar configuration produces delocalized and therefore metastable solute radical cations (Equation (4a)] which deprotonate in a few hundred nanoseconds, causing the delayed phenoxyl radical component.

Sesamol. As shown in Fig. 7, in the planar structure the three highest doubly occupied MOs (HOMO, HOMO-1, HOMO-2) have π-symmetry with strongly delocalized electrons but HOMO-3 shows n-symmetry. Rotation of the phenolic OH group with respect to the molecular plane changes the relative energy levels of these HOMOs (Fig. 7). The rotation of the OH group reduces the energy of HOMO-2 (planar structure) and increases the energy of HOMO-3 (planar structure) to an extent that in the perpendicular structure their relative poisitions are

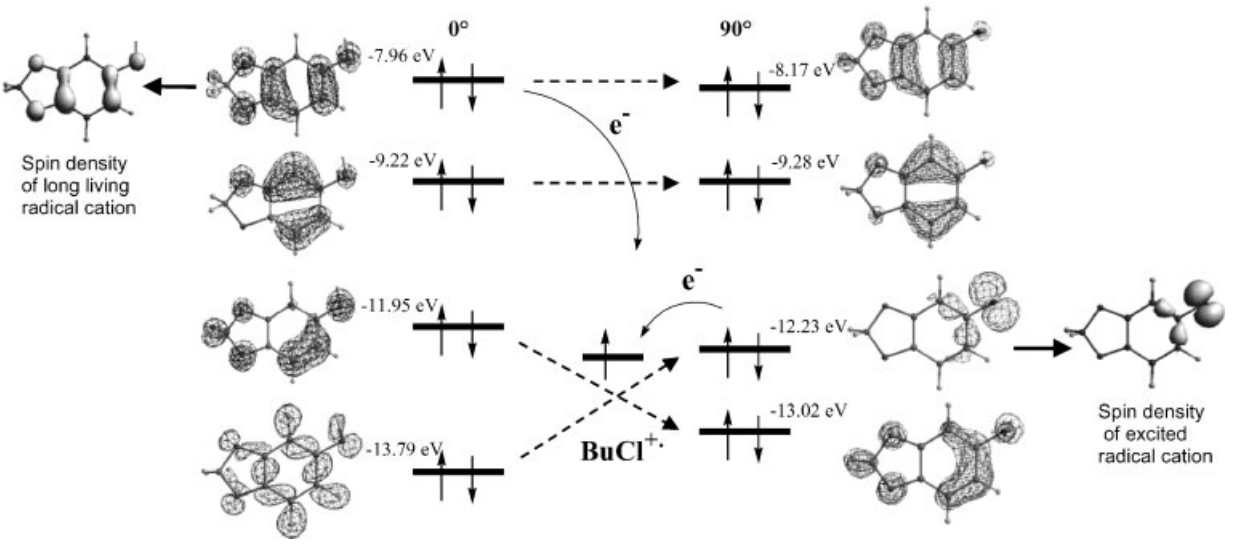

Figure 7. Transformations of the MOs of sesamol ground-state singlet depending on the molecular structure (OH group rotation) leading to different products by free electron transfer to $BuCl^{+\cdot}$, namely long-living (stable) radical cation and very short-living (excited) radical cation. MO energies were calculated with HF/6–1G(d)//B3LYP/6–31G(d); isocontour = 0.05

inverted. The HOMO-2 and HOMO-3 at 0° roational angle (planar configuration) become HOMO-3 and HOMO-2 at 90° rotation (perpendicular configuration), respectively. In the perpendicular conformation, the energetic distance between HOMO and HOMO-3 is reduced by ~1 eV. Furthermore, in the perpendicular conformation, HOMO, HOMO-1 and HOMO-3 are delocalized but the HOMO-2 is strongly localized on the oxygen atom. Considering the MO scheme of a neutral closed shell sesamol molecule, electron transfer from HOMO, HOMO-1, HOMO-2 of the planar conformation and from HOMO-2 of the perpendicular conformation can produce ground-state and excited-state configurations (Koopman's configurations) of the corresponding radical cation. A comparison of the planar and perpendicular ground-state structures (Fig. 7) suggests that a delocalized long-lasting radical cation can be obtained by ionizing the planar structure, whereas ET from the perpendicular configuration generates an unstable radical cation. In the perpendicular conformation, because of the excess energy and the very efficient overlapping of the HOMO-2 with the orbital of the solvent radical cation, the electron transfer can take place. According to the frontier orbital theory, the interaction energy between electron donor and acceptor increases with increasing overlapping of the orbitals and reduction of the energy gap of the MOs.[25,26] This provides the rational for the electron transfer from HOMO-2 in the perpendicular conformation, producing the sesamol radical cation with spin localized on the oxygen atom of the OH group. This should be an extremely short-lived species having a lifetime much shorter than the experimental time resolution (<5 ns) which immediately deprotonates to give the sesamol radical.

Trolox and curcumin. Compared with sesamol, these molecules also follow similar changes in the highly occupied HOMOs energy levels and separation upon rotation of the OH group with respect to the molecular plane. Therefore, similar electron transfer mechanism which simultaneously produces solute radical cations and oxyl radicals is envisaged. Quantum chemical calculations for trolox and curcumin are more complicated because of the larger number of MOs and could not be done in detail. A high rotational energy barrier for the phenolic OH group should increase the $ArOH^{\cdot+}/ArO^{\cdot}$ ratio. The intramolecular hydrogen bonding in the case of curcumin can possibly prevent a free rotation of the OH group. As a consequence, the equilibrium between all possible rotamers is shifted to nearly planar conformers, which produce mostly long-living cation radicals. Other parameters obtained by quantum chemical calculations for $SOH^{\cdot+}$, $COH^{\cdot+}$ and $TOH^{\cdot+}$ are also summarized in Table 2. It should be noted that the O—H bond length of the enolic group of curcumin is increased to 1.01 Å compared with the O—H bond length of the phenolic group (0.9 Å) owing to intramolecular hydrogen bonding making the molecule planar.

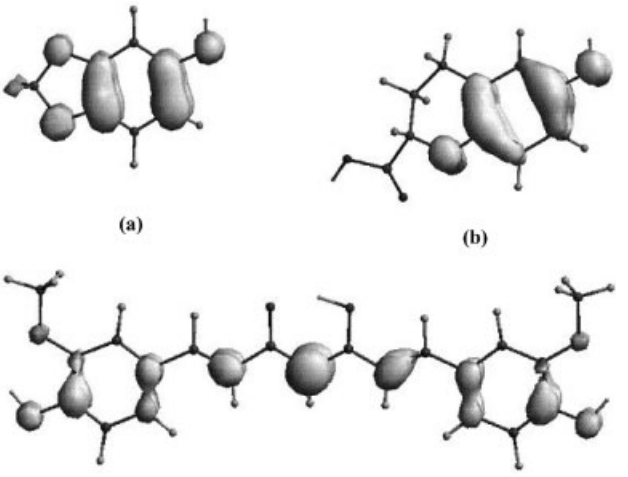

Figure 8. Spin density distribution of the long-lived radical cations: (a) sesamol, (b) trolox and (c) curcumin [B3LYP/6–31G(d), isospin = 0.003]

Additionally, the lifetime τ of $ArOH^{\cdot+}$ of the longer lived metastable cation radicals of sesamol, trolox and curcumin depends on the spin density at the phenolic oxygen atom [*S*(O)]. The calculated spin density S(O) and Δq(OH) difference of Mulliken charges at the OH group between the cation radical and the singlet ground state (as shown in Fig. 8 and Table 2) is highest for $TOH^{\cdot+}$ and lowest for $COH^{\cdot+}$. This agrees well with the radical cation lifetimes of these solutes, COH (3.33 μs) > SOH (2.22 μs) > TOH (0.91 μs). An inverse correlation between the τ value of the solute radical cation and the spin density or Mulliken charges at the phenolic oxygen atom is observed, as is the case for other phenolic compounds.[23] This clearly demonstrates that higher spin density on the phenolic oxygen atom results in a decrease in the τ value of the corresponding cation radical.

Mechanistic aspects

As stated earlier and within a simplified picture, the electron transfer takes place from both the planar and the perpendicular conformation of the ground-state phenols. Futhermore, the high gas-phase solute–solvent ionization potential differences give reason for an unhindered electron transfer step in a short time-scale where the molecule could be imagined as a frozen state.

On this basis, two borderline radical cation conformers are formed with very different tendencies for deprotonation after ionization, according to Eqns (4a) and (4b). In the FET from the planar structure, the radical cations have delocalized electrons and therefore exhibit lifetimes of several hundred nanoseconds [Eqn (4a)]. In the FET from the perpendicular structure, the radical cation with spin and charge localized on the oxygen alone represents a very unstable species with a lifetime much shorter than nanoseconds, which dissociates immediately to a

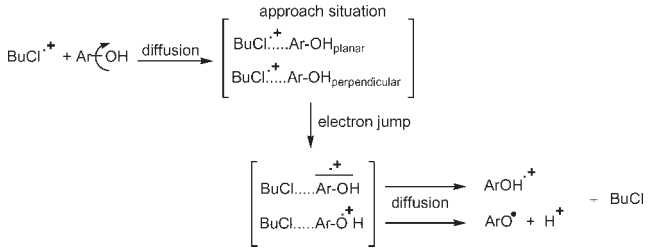

Scheme 2

phenoxyl radical [Eqn (4b)]. It has been shown earlier that $\log(1/\tau)$ of the solute radical cation of various phenols increase with the spin density S(O) and the difference of Mulliken charges at the OH group between the cation radical and the singlet ground state Δq(OH).[23] The same trend between $\log(1/\tau)$ (or τ) and S(O) or Δq(OH) is observed for the radical cations of SOH, TOH and COH (Table 2). This consolidates the assumed reaction mechanism and rate constants. The data show that the methylendioxy substituent of sesamol and π-delocalization of curcumin impart more stability to their cation radicals as compared with even naphthols.[23]

The rate constants obtained for the free electron transfer (2) from SOH, COH and TOH to $BuCl^{\cdot+}$ (Table 1) are of the order found also for other phenol derivatives, i.e. they are diffusion controlled.[8,12] This holds also for the electron transfer quenching of $ArOH^{\cdot+}$ by TEA. Considering the single steps of the FET (Scheme 2) it should be stated that diffusion is the slowest one whereas the electron jump itself is a completely unhindered and therefore very rapid process. Hence, in each encounter of the reactants the electron jump happens at the first approach (collision). This seems to be the real reason for the reflection of the rotation conditioned conformers observed experimentally; see reaction channels of the FET (4).

In this paper, it was not intended to analyse in depth the influence of distinct modes of molecule oscillations on the electron transfer mechanism, which has been reported previously.[7] This product ratio of FET (4) involving the actual natural phenols studied here, with 57–62% of $ArOH^{\cdot+}$, only a slightly higher yield compared with the 50% $ArOH^{\cdot+}$ contribution for the 'simple' phenols[7] has been found. This could mean that on the one hand the alkoxyl groups in *ortho*- and *para*-positions stabilize the cations by the well-known electron-donating effect. On the other hand, and more convincing, the rotating bond (C—OH) exhibits in these cases a higher rotation barrier. This is indicated by the quantum chemical calculations at least for COH and TOH.

The deprotonation kinetics (k_6) of $ArOH^{\cdot+}$ follows the order TOH > SOH > COH, which agrees well with the spin density S(O) and the difference in Mulliken charges at the OH group between cation radical and singlet ground state Δq(OH)[27] (Table 2). It should be noted that S(O) and Δq(OH) are a measure of the transient stabilities.

For the phenoxyl radicals, a comparison of its decay rates ($2k_7$) shows that $TO^{\cdot}$ decays more slowly than $SO^{\cdot}$ and $CO^{\cdot}$. Overall, in the FET, the phenols SOH, COH and TOH (which stand for other naturally occurring phenols) exhibit relatively higher yields of radical cations [reaction (4a)] than the phenoxyl radicals [reaction (4b)]. Furthermore, the stability of the radical cations derived from the natural phenols was found to be considerably higher than those of other phenols.[7,27] This can be derived from the deprotonation rates (lifetimes) given in Table 2.

CONCLUSIONS

Sesamol, curcumin and trolox react with solvent cation radicals, like other phenols, to produce simultaneously phenol radical cations and phenoxyl radicals. This is followed by a delayed deprotonation of the metastable phenol radical cation resulting in a delayed formation of the phenoxyl radical. The peculiarities of the kinetics and mechanism of the ionization of these compounds in non-aqueous systems depends, to a large extent, on the substituents, i.e. the *p*- and *o*-alkoxyl groups are very effective stabilizing factors. A good correlation is observed between the experimatal data (lifetime, $ArOH^{\cdot+}/ArO^{\cdot}$ ratio) and the theoretically calculated data S(O), Δq(OH) and activation energies for the OH group rotation.

REFERENCES

1. Vincow G. In *Radical Ions*, Kaiser ET, Kevan L (eds). Wiley: New York, 1968; 151–209.
2. Mehnert R. In *Radical Ionic Systems—Properties in Condensed Phases*, Lund A, Shiotani M (eds). Kluwer: Dordrecht, 1991; 231–284.
3. Brede O, Mehnert R, Naumann W. *Chem. Phys*. 1987; **115**: 279–290.
4. Guldi DM, Asmus K-D. *J. Am. Chem. Soc*. 1997; **119**: 5744–5745.
5. Mehnert R, Brede O, Naumann W. *Ber. Bunsen-Ges. Phys. Chem*. 1982; **86**: 525–529.
6. Lide DR (ed.). *CRC Handbook of Chemistry and Physics*. CRC Press: Boca Raton, FL, 1992.
7. Brede O, Hermann R, Naumann W, Naumov S. *J. Phys. Chem. A*. 2002; **106**: 1398–1405.
8. Brede O. *Res. Chem. Intermed*. 2001; **27**: 709–715.
9. Brede O, Orthner H, Zubarev V, Hermann R. *J. Phys. Chem*. 1996; **100**: 7097–7105.
10. Hermann R, Dey GR, Naumov S, Brede O. *Phys. Chem. Chem. Phys*. 2000; **2**: 1213–1220.
11. Mahalaxmi GR, Hermann R, Naumov S, Brede O. *Phys. Chem. Chem. Phys*. 2000; **2**: 4947–4955.
12. Brede O, Ganpathi MR, Naumov S, Naumann W, Hermann R. *J. Phys. Chem. A*. 2001; **105**: 3757–3764.
13. Brede O, Hermann R, Naumov S, Perdikomatis GP, Zarkadis AK, Siskos MG. *Chem. Phys. Lett*. 2003; **376**: 370–375.
14. Braun W, Herron JT, Kahaner DK. *Int. J. Chem. Kinet*. 1988; **20**: 51–62.
15. Frisch MJ, Trucks GW, Schlegel HB, Scuseria GE, Robb MA, Cheeseman JR, Zakrzewski VG, Montgomery JA Jr, Stratmann RE, Burant JC, Dapprich S, Millam JM, Daniels AD, Kudin KN, Strain MC, Farkas O, Tomasi J, Barone V, Cossi M, Cammi R, Mennucci B, Pomelli C, Adamo C, Clifford S, Ochterski J,

Petersson GA, Ayala PY, Cui Q, Morokuma K, Salvador P, Dannenberg JJ, Malick DK, Rabuck AD, Raghavachari K, Foresman JB, Cioslowski J, Ortiz JV, Baboul AG, Stefanov BB, Liu G, Liashenko A, Piskorz P, Komaromi I, Gomperts R, Martin RL, Fox DJ, Keith T, Al-Laham MA, Peng CY, Nanayakkara A, Challacombe M, Gill PMW, Johnson B, Chen W, Wong MW, Andres JL, Gonzalez C, Head-Gordon M, Replogle ES, Pople JA. *Gaussian 98 (Revision A.11)*. Gaussian: Pittsburgh, PA, 2001.
16. Becke AD. *J. Chem. Phys*. 1993; **98**: 5648–5662.
17. Becke AD. *J. Chem. Phys*. 1996; **104**: 1040–1046.
18. Lee C, Yang W, Parr RG. *Phys. Rev. B* 1987; **37**: 785–789.
19. Brede O, Naumov S, Hermann R. *Radiat. Phys. Chem*. 2003; **67**: 225–230.
20. Shida T. In *Electronic Absorption Spectra of Radical Ions*. Elsevier: Amsterdam, 1988; 12ff.
21. Khopde SM, Priyadarsini KI, Venkatesan P, Rao MNA. *Biophys. Chem.* 1999; **80**: 83–89.
22. Cadenas E, Merenyi G, Lind J. *FEBS Lett*. 1989; **253**: 235–238.
23. Hermann R, Naumov S, Mahalaxmi GR, Brede O. *Chem. Phys. Lett*. 2000; **324**: 265–272.
24. Brede O, Kapoor S, Mukherjee T, Hermann R, Naumov S. *Phys. Chem. Chem. Phys*. 2002; **4**: 5096–5104.
25. Klopman G. *J. Am. Chem. Soc*. 1968; **90**: 223–234.
26. Salem L. *J. Am. Chem. Soc*. 1968; **90**: 543–552.
27. Ganapathi MR, Naumov S, Hermann R, Brede O. *Chem. Phys. Lett.* 2002; **337**: 335–340.

